RESEARCH PAPER

HOLOCENE COASTAL PROCESSES OF AN UPLIFTED FENNOSCANDIAN COAST: A CASE STUDY FROM THE TURIY PENINSULA (THE NORTHERN COAST OF THE WHITE SEA)

Alena P. Yakovleva[1*], Tatiana Yu. Repkina[1], Nataliya E. Zaretskaya[1,2], Olga S. Shilova[3], Fedor A. Romanenko[3]
[1]Institute of Geography RAS, Staromonetniy lane, Moscow, 119017, Russia
[2]Geological Institute RAS, Pyzhevsky lane, Moscow, 119017, Russia
[3]Lomonosov Moscow State University, Faculty of Geography, Leninskie Gory, Moscow, 119991, Russia
*Corresponding author: iakovleva-ap@yandex.ru
Received: August 9th 2025 / Accepted: March 8th 2026 / Published: June 30th 2026
https://doi.org/10.24057/2071-9388-2026-4200

ABSTRACT. This study examines coastal processes and resulting morphologies during the Holocene on the Turiy Peninsula (the southern part of the Kola Peninsula). The genetic classification of the modern coasts revealed both wave- and non-wave-dominated types. Similar patterns were also identified on elevated paleocoastlines. Four geomorphological levels of the Turiy Peninsula were distinguished, considering their age and environmental settings based on field observations, interpretation of satellite images, topographic data, drilling cores, radiocarbon dating, and diatom analysis. The Turiy Peninsula provides a unique setting for paleogeomorphological research due to the good preservation of coastal landforms and the diversity of geomorphological settings. This well-preserved coastal morphology is attributed to relatively high Holocene uplift rates, which caused rapid exposure of the coasts beyond the zone of active wave impact. As such, the area represents a sensitive archive of postglacial coastline response to glacioisostatic uplift in formerly glaciated shield environments. Radiocarbon dating and diatom analysis of sediments from isolated basins allowed us to estimate the regional uplift rate over the last 3.5–4 cal kyr at 5–7 mm/year. These rates are significantly higher than the uplift rates observed in adjacent areas for the same period, supporting the interpretation of block-structured tectonic movements in the region.

KEYWORDS: coastal morphodynamics, sea level changes, diatoms, radiocarbon dating, the Holocene, Kola Peninsula coast

CITATION: Yakovleva A. P., Repkina T. Yu., Zaretskaya N. E., Shilova O. S., Romanenko F. A. (2026). Holocene Coastal Processes of an Uplifted Fennoscandian Coast: a case study from the Turiy Peninsula (the northern coast of the White Sea). Geography, Environment, Sustainability, 2 (19), 84-95
https://doi.org/10.24057/2071-9388-2026-4200

ACKNOWLEDGEMENTS: Paleogeomorphological studies of this research were funded by the Institute of Geography RAS (FMWS-2026-0001). Drilling of lacustrine-marsh sediments and diatom analysis were carried out according to the State Programs of the Lomonosov Moscow State University (121040100323-5 and 121051100167-1, respectively). Radiocarbon dating was conducted in the framework of the State Assignment of the Geological Institute RAS (FMMG-2022-0002). The authors express their deepest gratitude to Dmitry V. Korzinin (Shirshov Institute of Oceanology RAS) and students of the Department of Geomorphology and Paleogeography of the Faculty of Geography MSU for assistance in field research. The authors are grateful to the administration of the Kandalaksha Reserve for the opportunity to conduct research in the protected area.

Conflict of interests: The authors reported no potential conflict of interests.

INTRODUCTION

Since the end of the Last Glaciation, the coasts of Fennoscandia, and the Kola Peninsula in particular, have experienced relative sea level (RSL) fall (Koshechkin 1979; Korsakova and Kolka 2017; Baranskaya et al. 2018). This was a result of rapid isostatic land uplift that followed the retreat of the Scandinavian ice sheet (Lavrova 1960; Hughes et al. 2016). This initiated coastal processes (such as coastline progradation, coastal erosion, beach-ridge formation, etc.) that gave rise to diverse morphogenetic shore types.

Sequences of transgressive and regressive events preserved in coastal morphology offer critical insights into coastline evolution. Their reconstruction relies on coastline elevation data, morphostratigraphic indicators (e.g., number of beach ridges), and sedimentological markers (Zenkovich 1962).

In the White Sea region, deglaciation took place between ~17 and 11 cal ka BP (Demidov et al. 2006; Hughes et al. 2016; Stroeven et al. 2016; Astakhov et al. 2016). Kandalaksha Bay is the area where it occurred later than in other regions of the White Sea. The precise timing of deglaciation in this area remains debated. It is currently assumed that deglaciation was completed here between ~12.5 and 11 cal ka BP (Astakhov et al. 2016; Astafiev et al. 2012; Evzerov et al. 2007; Korsakova et al. 2023). Initial ingress of marine waters in the eastern part of Kandalaksha Bay occurred ~13.8–12.4 cal ka BP (Kolka et al. 2013, 2015, 2016; Polyakova et al. 2023). The main stages of the postglacial evolution of the White Sea are as follows: Late Glacial transgression (~13.4–11.6 cal ka BP), rapid RSL fall/regression (~11.6–9.5 cal ka BP), an Early-Middle Holocene highstand, or the Tapes transgression (~9.5–6.8 cal ka BP), and subsequent RSL fall to the present level (Korsakova 2022). The RSL highstand reached its maximum, particularly in the apex of Kandalaksha Bay (Kolka and Korsakova 2017; Korsakova 2022).

The highest dated coastlines there reach up to 100 m a.s.l. (Baranskaya et al. 2018) or 120 m a.s.l. (Korsakova 2022). For comparison, on the Zimniy Coast of the White Sea, the highest coastlines do not exceed 14–20 m a.s.l. (Shilova et al. 2019). The uplift rate generally decreases along the northwest-southeast gradient, reflecting increasing distance from the center of the Last Glacial ice sheet (Lavrova 1960; Korsakova and Kolka 2017).

Block vertical movements along faults are superimposed on the general uplift of the Baltic Shield (Baranskaya et al. 2018; Korsakova 2022; Shvarev 2022). The Turiy Peninsula represents one of these blocks (Shvarev 2022) and displays a diverse set of coastal landforms and uplift levels. Investigating this site may provide insights into the spatial heterogeneity of postglacial movements within the Baltic Shield.

As a result of differential isostatic uplift, tectonic activity, and variations in sediment supply, the configuration of the White Sea coastline, especially within Kandalaksha Bay, changed rapidly and unevenly throughout the postglacial period, reflecting spatial variability in uplift intensity and local conditions. This led to changes in coastal processes in different parts of the coast.

This study aims to reconstruct the evolutionary stages of the Turiy Peninsula coast and to identify the key geomorphological factors that led to the formation of specific coastal morphologies in the Holocene. We conducted paleogeomorphological and lithostratigraphic studies of the Turiy Peninsula coastal topography, supported by the results of radiocarbon dating and diatom analysis.

REGIONAL SETTING AND CURRENT STATE OF THE ART

The Turiy Peninsula is located in the southern part of the Kola Peninsula and protrudes into Kandalaksha Bay of the White Sea. Its geological composition is rather homogeneous. Most of the peninsula is mantled by Quaternary sediments, which occupy various altitudinal zones across the area (Astafiev et al. 2012; Kolka et al. 2013). They are represented by a discontinuous cover of glacial, glaciofluvial sediments (sand with boulders, pebbles and gravel), marine sediments of the Late Glacial transgression (clays, rarely silts, sands, sands with pebbles) and Holocene marine sediments (silts, sands, less frequently pebble and boulder-pebble deposits, silts and clays). Only the extreme south of the Turiy Peninsula consists of Caledonian rock formations (Astafiev et al. 2012).

Despite the overall geological homogeneity, coastal morphology differs markedly between the northwestern and southeastern sectors due to contrasting hydrometeorological conditions. The highest wave energy occurs during winds from the southeast and south (Terziev et al. 1991). The maximum wave height reaches 2 m within the SE and S coasts and does not exceed 1 m on the NW coast (Arkhipkin et al. 2015). Kandalaksha Bay of the White Sea is a subarctic basin that remains ice-covered for 6–7 months annually. However, quasi-stationary ice-free zones often form due to prevailing winds from the southeast and south. This creates conditions for wave action to impact the coasts of this part of the peninsula even within the ice-covered season (Terziev et al. 1991). Additionally, the nearshore slope morphology of the peninsula coasts is not uniform (Nikiforov et al. 2012). The NW coast (within Sosnovaya Bay) has a shallow shoreface, which is largely sheltered from wave impact. Tides are the primary driver of coastal change in this area. The SE and S coasts have a steeper shoreface and a spatial position favoring intense wave action. This combination of factors shapes the present coastal dynamics of the peninsula and probably influenced them in the past.

The coastal dynamics of the Turiy Peninsula have not been previously investigated. Nevertheless, some topographic profiles provide information on the morphology of the southeastern part of the peninsula (Kolka et al. 2013). Studies on the classification of the Turiy Peninsula coasts are scarce. Existing small-scale maps of coastal types for the Kola Peninsula and the White Sea (Safianov and Solovieva 2005; Yermolov 2010) do not allow for detailed zoning of the Turiy Peninsula coasts and uplifted land areas. Furthermore, RSL and paleogeographical reconstructions are available for adjacent territories (Umba, Kuzreka, Kanozero Lake) (Evzerov et al. 2007; Kolka et al. 2013; Grekov et al. 2013a,b; Sapelko et al. 2022; Ludikova et al. 2022). This provides a basis to compare evolutionary stages between the Turiy Peninsula and adjacent areas.

MATERIAL AND METHODS

We conducted field investigations in the northwestern (southern coast of Sosnovaya Bay) and southeastern parts of the Turiy Peninsula to reconstruct the peninsula's coastal morphodynamics and RSL fluctuations during the Holocene (Fig. 1).

Applying the principles of uniformitarianism, we interpreted the uplifted terrain through comparison with contemporary coastal morphology. The geomorphological subdivision of the area follows classical concepts of coastal morphogenesis based on the morphology of beach ridges and marine terraces, following the approach of Zenkovich (1967), Kaplin et al. (1991), and Bird (2008). The presence, number, and morphology of beach ridges, together with a straight coastline planform, indicate that wave-dominated processes (depositional and erosional) control coastal evolution. An uneven coastal bench and an indented coastline outline show that non-wave processes, often tidal, dominate the system. Rock cliffs characterize structurally primary rocky shores that are almost unchanged by wave processes.

Geomorphological studies included topographic profiling, GPS logging, and detailed description of landforms at slope transitions. Photographic documentation supplemented the field observations. Relative elevation measurements with an estimated accuracy of a few centimeters were made using a *CST Berger 17-632 Hand Sight Level* with a measuring rail. Distances were measured using the *Garmin GPSMAP 62s portable navigator* (error of ±5 m).

We used the isolation-basin method to reconstruct RSL fluctuations. Postglacial isostatic uplift forms these basins and allows us to date former coastline positions at a common elevation. Isolation basins are widely used in reconstructions of RSL changes (Donner et al. 1977; Evzerov et al. 2007;

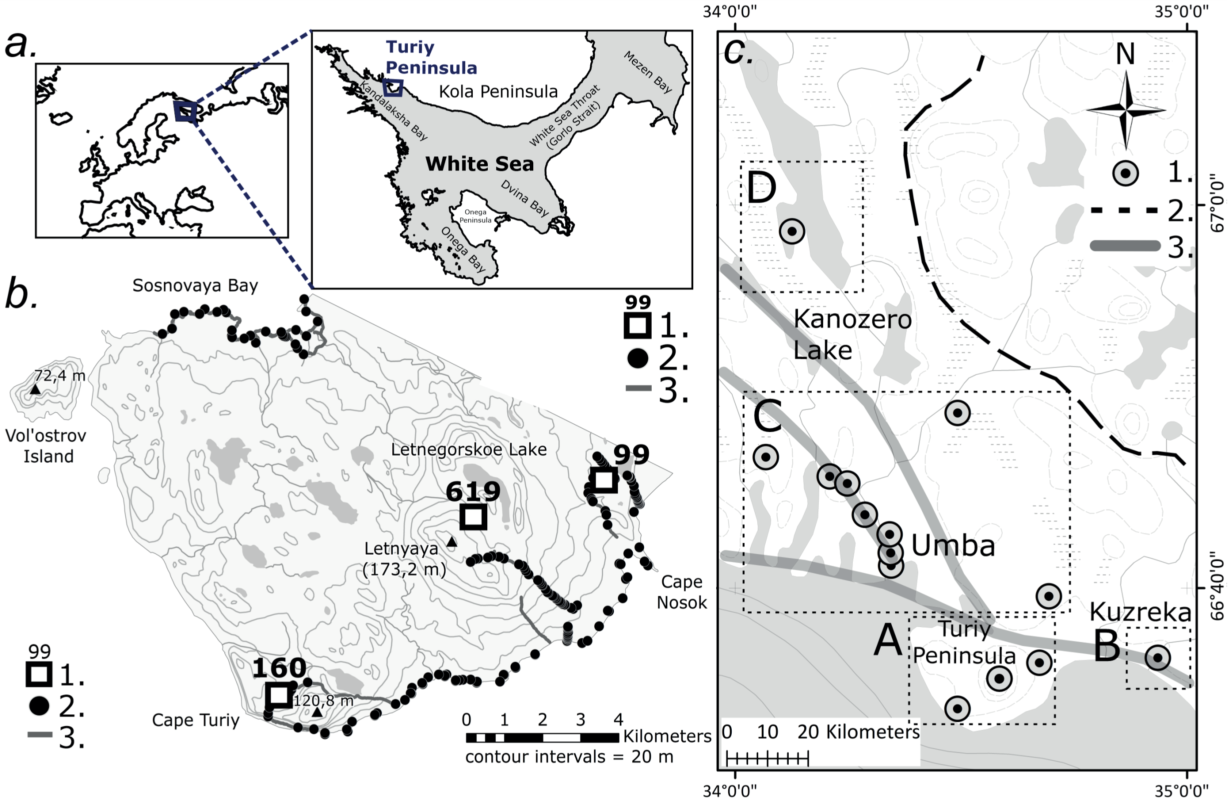

Fig. 1. Study area and current state of the art. Legend: a. Location of the study area; b. Map of the field data: 1 – positions of boreholes (boreholes are signed with numbers), 2 – points of geological and geomorphological observations, 3 – location of routes and profiles; c. The state of paleogeographic knowledge of the Turiy Peninsula and adjacent territories: A – this research, B – Grekov et al. 2013, C – Kolka et al. 2013, D – Ludikova et al. 2022; Sapelko et al. 2022; 1 – points of geological-geomorphological research, 2 – proposed boundary of the Scandinavian Ice Sheet, Salpausselkä stage I, which correlates with the Younger Dryas (Astafiev et al. 2012; Korsakova et al. 2023), 3 – elements of the fault-block structure according to (Shvarev 2022).

Subetto 2009; Baranskaya et al. 2018; Korsakova 2022). Within them, a change in sedimentation regime occurs in several stages from brackish to freshwater. Currently, some of these lakes have become freshwater, while others remain waterlogged. Establishing the time of transition from marine to freshwater conditions in these basins was among the objectives of our research.

Three sediment cores (99, 160, 619; see Fig. 1) were collected from isolated basins using a *Hiller peat corer* to study sedimentary successions. The cores are located at elevations of 21.5, 29.5, and 98 m a.s.l., respectively (cores 99, 160, and 619). We collected cores from lakes near the paleo coastlines and from the summit surface to define the upper limit of marine transgression. The sampling was supplemented with lithostratigraphic descriptions. The sampling strategy targeted lithological boundaries and intervals with elevated plant and detrital content for sediment column analysis. The composition of the sediments recovered in the cores appears in Fig. 5 and in Section 4.2.

Boundaries of lithostratigraphic units were targeted for radiocarbon dating (6 dates, Fig. 5, Table 1). Radiocarbon dating was performed using a standard A-B-A procedure of sample pretreatment applied in the Laboratory for Isotope Geochemistry and Geochronology of the Geological Institute of RAS (GIN-index), described in Zaretskaya et al. (2001; 2007). For measurement of 14C activity in the sample, the liquid scintillation counting (LSC) technique was applied. The obtained dates were calibrated using the Calib 8.2 calibration software based on the IntCal20 calibration curve (Reimer et al. 2020).

Diatom analysis of sediments was performed for cores 99 (4 samples), 160 (12 samples), and 619 (5 samples) in the Laboratory of Geoecology of the North, Faculty of Geography, MSU. Since the number of diatoms in cores 99 and 619 was insufficient, we constructed the diagram only for core 160 (Fig. 6). We collected samples at 10-cm intervals and paid special attention to lithological boundaries that likely mark shifts in depositional conditions.

The processing of samples for diatom analysis was carried out according to the standard procedure (Diatoms of the USSR... 1974): dry sediments were treated with hot hydrogen peroxide (H_2O_2) for 1 h to destroy organic matter; then the samples were washed with distilled water until full removal of H_2O_2. Permanent slides were prepared on a Naphrax mountant with a refractive index of 1.68. Diatoms were studied under an Axiostar Plus light microscope (Zeiss) with the magnification of ×1000. At least 300 valves were identified to the species level in each sample. The number of diatom valves per 1 g of air-dry sediment was calculated (Davydova 1985). The diatom diagram was plotted using the C2 v. 1.7 software. The names of taxa are given in accordance with AlgaeBase (Guiry and Guiry 2025).

The limited diatom content in the cores resulted in a small sample set. The diatom data served as supplementary evidence, while paleogeomorphological and remote-sensing analyses formed the core of the study.

Geomorphological units (Fig. 2) were identified based on field observations, interpretation of Landsat and QuickBird satellite images (spatial resolution: 15–30 m and 2.4 m, respectively), and digital elevation models (DEMs) or digital surface models (DSMs), in particular, ArcticDEM. It is an automatically produced high-resolution, high-quality digital surface model (DSM) of the Arctic using optical stereo imagery, high-performance computing, and open-source photogrammetry software (spatial resolution: 2 m; Porter et al. 2023). Also, we used relative-elevation measurements and core data. Mapped units were classified based on the degree of erosion, genetic type, and relative age according to standard geomorphological criteria (Zenkovich 1967; Kaplin et al. 1991; Bird 2008).

RESULTS

Surface topography as an indicator of coastal processes in the Holocene

Based on field observations and remote data (satellite imagery, DEMs), we identified three distinct coastal sectors of the modern Turiy Peninsula (Fig. 2): the southeastern, southwestern, and northwestern (within Sosnovaya Bay).

The *southeastern* sector, exposed to prevailing SE winds, is characterized by sea cliffs and sandy or pebbly beaches. The coast in this part is composed of rocks less resistant to erosion (loose, unconsolidated deposits – usually sands, less often pebbles). This sector shows an alternating pattern: cliffs prevail on headlands, while beaches are found in bays. Sandy and pebbly-sandy shores are formed with a sufficient volume of fine-grained sediments. Where the supply of fine sediments is limited and glacial material dominates, coarse pebble and boulder-pebble shores are formed. In the northeastern extension of this sector, sandy and pebbly-sandy beaches prevail. This pattern occurs in areas where the sandy tidal flat reaches 50 m in width, and the beach is about 10 m wide.

In the *southwest*, crystalline intrusive rocks resist coastal erosion, and the coastline remains largely unaffected by marine processes. The height of the cliff at Cape Turiy reaches 60–63 m.

The *northwestern* coast is protected from wave action, and tidal flats of various lithologies are common. The width of the tidal flat reaches its maximum (150–200 m) in the apex of Sosnovaya Bay. The coast here is composed mainly of silts enriched in organic detritus.

The modern coast of the Turiy Peninsula provides a clear reference for interpreting the genesis of coastal landforms. Because contemporary coastal forms and the morphology of the uplifted terrain share the same genetic origin, we use modern coastal processes as an analogue for understanding the development of the raised surfaces. The staircase of different-age coastal landforms

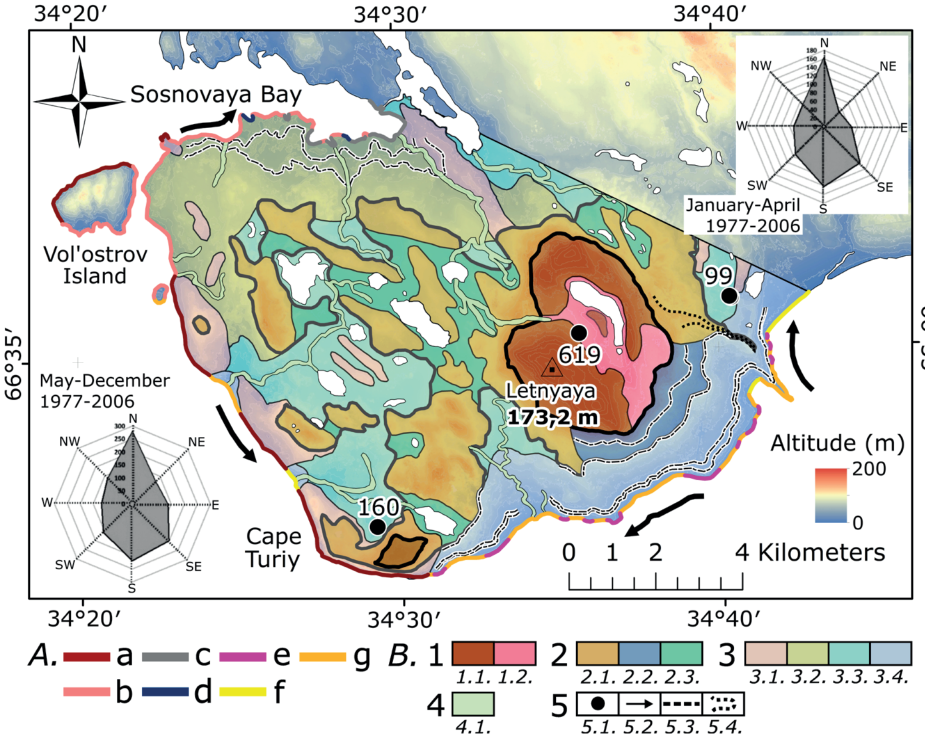

Fig. 2. Geomorphological map of the Turiy Peninsula coast A. Modern coastal types: shores almost unchanged by wave processes: a. primary rocky shores; shores shaped by non-wave processes: tidal shores with different lithology of tidal flat: b. boulder-rock, c. silt and sandy silt, d. mixed type; wave-induced shores: erosional: e. cliffs in sediments of marine terraces, depositional: f. sandy and pebbly-sandy beaches and lagoons, g. pebble and boulder-pebble beaches. B. Genetic types of landforms: 1. Surfaces without traces of coastal processes at heights of more than 90 m a.s.l.: 1.1. Structural landforms with fragmentary sediment cover, 1.2. Structural gently sloping plain partially overlain by glacial and glaciofluvial deposits; 2. Surfaces reworked by coastal processes during the Late Glacial transgression, and during the existence of the Early and Middle Holocene sea at altitudes of 50–90 m a.s.l.: 2.1. Structural ridges and massifs with fragmentary sediment cover, practically unchanged by wave processes, 2.2. Inclined wave-cut platforms transformed by coastal processes with a thin cover of marine sediments and a series of beach ridges, 2.3. Structural basins of paleostraits and bays filled with marine and lacustrine-marsh deposits; 3. Surfaces affected by coastal processes during the existence of the Middle-Late Holocene sea at altitudes less than 50 m a.s.l.: 3.1. Structural ridges and massifs with fragmentary sediment cover, practically unchanged by coastal erosion, 3.2. Stepped structural denudational surface transformed in the coastal zone with the predominance of non-wave processes (tides; shore-fast ice exposure; biogenic processes etc.) with a fragmentary sediment cover, 3.3. Structural basins of paleostraits and bays filled with marine and lacustrine-marsh deposits, 3.4. Inclined wave-cut platforms created by wave processes and composed of sand and gravel-pebble deposits, accompanied by a series of beach ridges; 4. Fluvial landforms formed after coastline retreat: 4.1. Slightly incised erosional landforms; 5. Other designations: 5.1. Positions of sediment cores, 5.2. Sediment flow direction, 5.3. Coastlines, 5.4. Separated structural ridges. Digital basis – 2-meter ArcticDEM (Porter et al. 2023). The wind rose indicates the frequency of wind directions according to the Umba hydrometeorological station for the periods of May-December and January-April 1977–2006 (ESIMO 2007)

on the southeastern terraces of the peninsula reflects this continuity and forms the basis for reconstructing Holocene coastline evolution. Analysis of the uplifted terrain shows that higher-level landforms closely replicate those found on the present coast, especially along the wave-exposed southeastern coastline, which preserves the most complete archive of coastal change.

We identified these coastal landforms at altitudes of 10, 22–23, 47–49, 69–70, and ~90 m a.s.l. Beach ridges at altitudes of up to 50 m a.s.l. are composed of sand and gravelly-sand sediment and mostly parallel the coastlines. A dense sequence of ridges at ~20 m a.s.l. (Fig. 3) suggests a period of intensified wave activity. Above ~50 m a.s.l., beach ridges become rarer and less distinct, with the highest traces of erosional modification observed at ~90 m a.s.l. on the southeastern slope of Letnyaya Mountain.

In the northwest of the peninsula, at comparable elevations (up to 90 m a.s.l.), the surface consists of irregular, poorly leveled marshy steps containing lakes, and remnants of glacial ridges. By their morphology, these surfaces resemble modern tidal flats. The scarps are not consistently expressed and occur at variable elevations, with the most distinct ones observed at 10 and 22 m a.s.l. The southern part of the peninsula forms a steep, nearly vertical rock scarp reaching up to 60–63 m a.s.l.

The summit surface of the peninsula, above 90 m a.s.l., consists of structural ridges and massifs and glacial features (Fig. 2). At these elevations, including the southeastern part of the peninsula, we did not identify any coastal landforms. Instead, we observed rounded boulders and clusters of boulders occurring at various heights (Fig. 3).

Morphological evidence implies that most of the peninsula once represented a skerry-type landscape, comprising bedrock islands and intervening straits (Fig. 4). Currently, these paleobays and paleostraits appear as gently sloping, waterlogged lowlands. This type of landscape is traditionally classified as a fiard-skerry (Safianov and Solovieva 2005).

Lithology and chronology of isolated lakes

We distinguished six lithological units in the studied sedimentary successions, as shown in Fig. 5. Core 99 is located at the extreme northeastern part of the peninsula

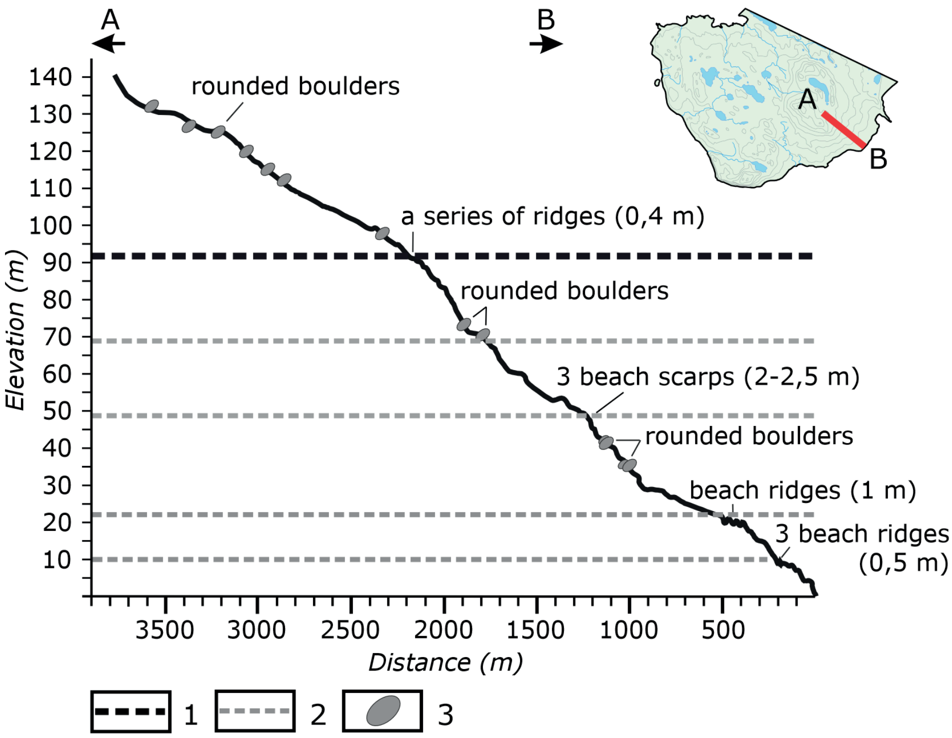

Fig. 3. Topographic profile of Letnyaya Mountain southeastern slope according to the results of field investigations: 1 – ancient coastlines, 2 – upper limit of the traces of wave reworking (erosional or accumulative), 3 – rounded boulders as indicators of marine or glacial impact

Fig. 4. Skerries of Kandalaksha Bay (vicinity of the Luvenga rural locality, Murmansk Region, NW Russia; photo by Alena Yakovleva)

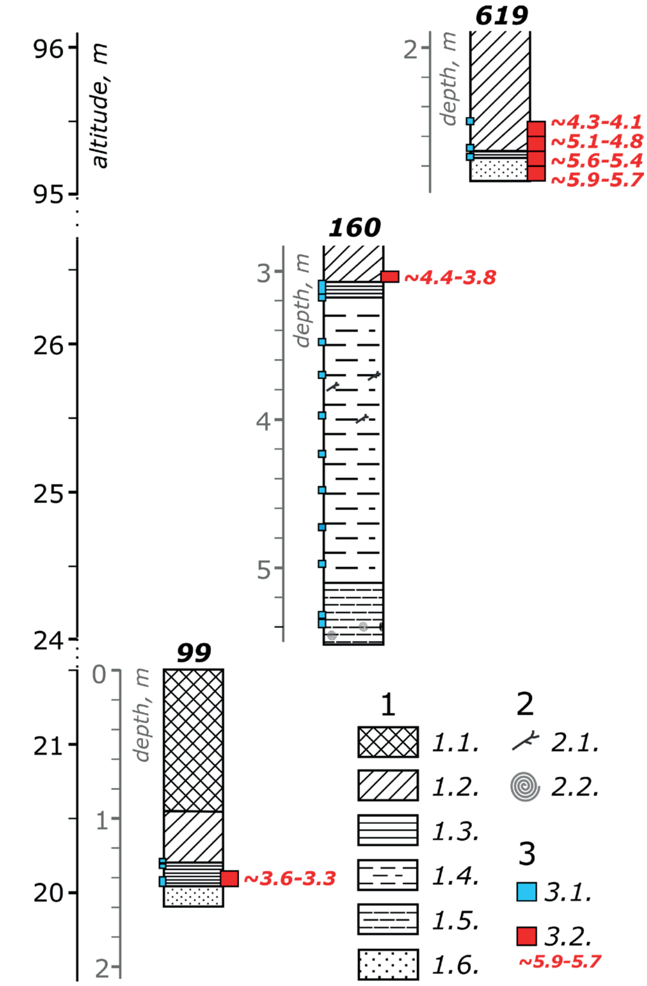

Fig. 5. Lithostratigraphy and chronology of the studied sediment cores: 1. lithological units: 1.1. – peat, 1.2. – silty peat, 1.3. – interbedding of silt and peat, 1.4. – silty gyttja, 1.5. – silt, 1.6. – sand, 2. organic detritus: 2.1. – shell detritus, 2.2. – plant detritus, 3. Other: 3.1. diatom sampling site, 3.2. radiocarbon sampling site and age in cal ka BP. The scale to the left from lithology shows the depth from the water surface (for sedimentary successions 99 (21.5 m a.s.l.), 160 (29.5 m a.s.l.), 619 (98 m a.s.l.)) and depth below the peat layer top in m.

at an elevation of 21.5 m a.s.l. The core was collected from a marshy surface that formerly represented a paleobay, separated from the sea by a beach ridge. The presence of the beach ridge confirms past marine influence at this level, as does the sediment succession revealed in the core. The core has a thickness of 1.6 m and exposes the following sedimentary sequence: beneath the lacustrine-marsh deposits, composed of peat and silty peat typical of freshwater lakes, we encountered sediments consisting of well-sorted sands. The transitional layer, represented by interbedding of peat and silt with sand, was selected for radiocarbon dating. It yielded an age of ~3.6–3.3 cal ka BP. Core 160 was taken from a low-lying, marshy part of the terrace at an elevation of 29.5 m a.s.l. It has a structure similar to that of core 99. This section is the most representative and has a thickness of 5.5 m. Its sedimentary succession, from top to bottom, includes peat, silty peat, interbedded peat and silt, silty gyttja with plant detritus, and silt. A radiocarbon age of ~4.4–3.8 cal ka BP was obtained from the transitional layer. Core 619 is located at an elevation of 98 m a.s.l. and was selected to determine the upper marine limit. Its thickness is 2.9 m. The upper two units are composed of lacustrine-marsh peat and silty peat. The top of the silty peat yielded radiocarbon ages of ~4.3–4.1 and ~5.1–4.8 cal ka BP. The transitional layer, represented by interbedded silt and peat, produced an age range of ~5.6–5.4 cal ka BP. The bottom of the section consisted of peaty sands and yielded an age of ~5.9–5.7 cal ka BP.

Below, we present the diatom assemblages from all three cores to examine past sedimentary conditions (Fig. 6).

The silty peat at the bottom of core 99 (1.45–1.33 m) contains diverse diatom associations (47 species per 300 valves) with high concentration (~80 million valves per gram). Chrysophyte cysts are present in smaller amounts of 3 thousand per gram. Diatoms are solely represented by freshwater species characteristic of small lakes with low electrolyte content and low pH values: *Stauroforma, Eucocconeis flexella, Eunotia* spp., *Brachysira* spp. In the gyttja (1.33–1.30 m), the diatom concentration is significantly higher – 1.5 billion valves per gram, and their taxonomic diversity is similar to the underlying layer (43 species per 350 valves). The most common species are *Stauroforma exiguiformis, Brachysira* spp., *Tabellaria* spp., and other species typical of northern dystrophic lakes.

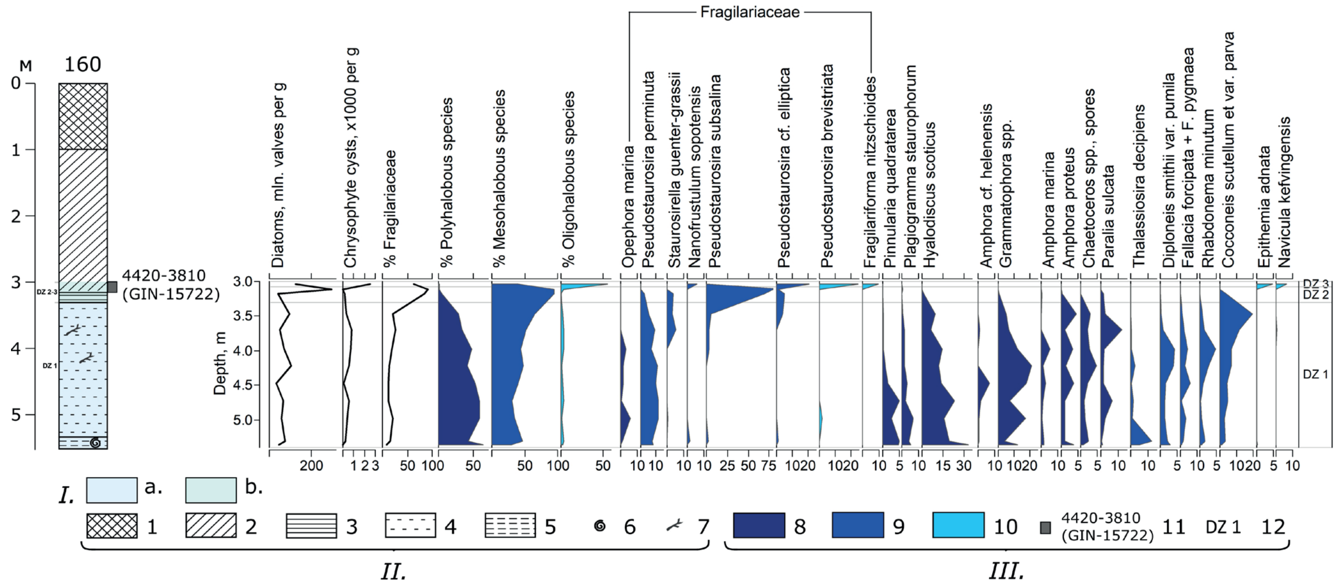

Fig. 6. Diatom diagram of core 160. I. Salinity: a. marine conditions, b. transitional (from marine to freshwater) conditions. II. Lithology: 1 – peat, 2 – silty peat, 3 – interbedding of silt and peat, 4 – silty gyttja, 5 – silt, 6 – shell detritus, and 7 – plant detritus. III. Characteristic of species according to Hustedt's halobous system (1957): 8 – polyhalobous, 9 – mesohalobous, 10 – oligohalobous. IV. Other: 11 – calibrated age, cal yrs BP, 2σ (95.4%), 12 – Diatom Zones (DZ)

The concentration of Chrysophyte cysts increases to 54 thousand per gram. Up the core, at the base of the peat layer (1.3–1.28 m), the number of diatom valves reaches its maximum (3 billion valves per gram) along with a sharp decline in taxonomic diversity (23 species per 400 diatom valves). The concentration of Chrysophyte cysts decreases to 9 thousand per gram. The dominant species are *Stauroforma exiguiformis* (74%) and *Aulacoseira alpigena. A. alpigena* is a cosmopolitan meroplanktonic species preferring oligotrophic water bodies with low electrolyte content. This species is widespread in the plankton of oligotrophic lakes and rivers of northern Europe, including the Kola Peninsula (Letanskaya 1974; Nikulina 1975; Kagan 2012).

Thus, we can conclude that all recorded species are freshwater ones. No species indicating a connection between the water body and the sea or proximity to the sea were revealed by diatom analysis of core 99. The species composition corresponds to a small dystrophic lake. The oligodominant nature of diatom associations with a very high concentration of valves and taxonomic diversity decreasing up the section provides evidence of lake overgrowth. The onset of the accumulation of organogenic lake sediments according to radiocarbon dating is 3640–3330 cal yrs BP (GIN-15721) (Table 1).

Diatom data from core 160 (29.5 m a.s.l.) are more representative (Fig. 6). Three DZs were distinguished based on diatom species composition and abundance. In DZ 1 covering the lower part of the section (5.4–3.3 m) the concentration of diatoms is high, varying between 30 and 100 million valves per gram. Chrysophyte cysts are found sporadically, in concentrations of less than 1000 cysts per gram. Taxonomic diversity of diatoms is 44–61 species per 300 valves. Diatom associations consist predominantly of marine and brackish-water benthic and meroplanktonic species: *Hyalodiscus scoticus, Thalassiosira decipiens, Paralia sulcata, Grammatophora* spp., *Amphora* spp., and *Pseudostaurosira perminuta*, among others. The proportion of polyhalobous species (according to the classification of Hustedt (1957)) decreases up the section (65–29%), while that of mesohalobous species increases from 29 to 66%.

DZ 2 (3.3–3.08 m) corresponds to the upper part of the bluish-gray silt, interlayered with peat beds. The concentration of diatoms increases from 40 to 300 million valves per gram with low taxonomic diversity, 24–16 species per 300 valves. Chrysophyte cysts are rare, <200 cysts per gram. The composition of diatom associations is monodominant: 70–84% of valves belong to *Pseudostaurosira subsalina*, a brackish-water species abundant on salt marshes and in microbial mats of the Baltic and North seas (Witkowski et al. 2000), where it is recognized as one of the best indicators of littoral and supralittoral environments. The total sum of small-cell brackish-water species of the Fragilariaceae family (*Pseudostaurosira subsalina, P.* cf. *elliptica, P. perminuta* and *Staurosirella guenter-grassii*) reaches up to 85–91% of all valves.

DZ 3 (3.08–3 m) corresponds to the basal part of the peat layer. The concentration of diatoms is high – 125 million valves per gram. Chrysophyte cysts have a significantly higher concentration than in the underlying sediments, equal to 2.5 thousand cysts per gram. Similar to DZ 2, small-cell species of the Fragilariacea family also predominate, but their share is lower (62%), and the composition is mixed: mesohalobous *Pseudostaurosira* cf. *elliptica* and *Nanofrustulum sopotensis* co-occur with oligohalobous *Pseudostaurosira brevistriata* and *Fragilariforma nitzschioides*. Oligohalobous *Navicula kefvingensis* and *Epithemia adnata* are also among the dominants. Taxonomic diversity is higher than in DZ 2 (38 species per 300 valves), which may be due to the mixing of the brackish-water and freshwater components of diatom associations.

Thus, the dominance of marine and brackish-water benthic species and the absence of holoplanktonic species among the dominants in DZ 1 indicate sedimentation in the relatively shallow coastal zone of the sea. The predominance of species with heavily silicified valves that are commonly attached to the substrate and are typical of the littoral zone with an active hydrodynamic regime points to sedimentation in the middle part of the tidal flat open to the sea. The mass development of small-cell colonial species of the Fragilariaceae family in DZ 2 indicates sedimentation in a calm hydrodynamic environment in shallow waters (Weckström and Juggins 2005; Repkina et al. 2023). Diatoms probably developed on macrophytes and in microbial mats in the upper part of the tidal flat, probably in lagoon environments. Marine depositional conditions are indicated by the continued dominance of brackish-water species and the minor presence of freshwater species. DZ 3 highlights transitional environments from marine to continental ones. This transition is dated to the time interval 4420–3810 cal yrs BP (GIN-15722) (Table 1).

In core 619 located at an altitude of about 98 m a.s.l. (Fig. 1) in the area of Lake Letnegorskoe, the horizon of dark

Table 1. Radiocarbon data and calibrated age estimations of the studied core sediments

#Core / #lithological unit (Fig. 5)	Altitude of the sampling point, m	Sampling interval, m	Laboratory code	14C date, yrs BP	Calibrated age, cal yrs BP, 2σ (95.4%), mean	Lithological description
99/4	21.5	1.45–1.35	GIN-15721	3240 ± 80	[3640–3330], 3460	Brownish silty peat with sand
160/3	29.5	3.15–3.05	GIN-15722	3720 ± 130	[4420–3810], 4070	Brownish silty peat
619/3.1	98	2.6–2.5	GIN-15918	3820 ± 30	[4300–4140], 4200	Dark brown peat with sand
619/3.2	98	2.7–2.6	GIN-15917	4390 ± 60	[5070–4840], 4970	Dark brown peat with sand
619/4-5	98	2.8–2.7	GIN-15916	4840 ± 40	[5610–5480], 5590	Dark brown peat with sand
619/5	98	2.9–2.8	GIN-15915	5090 ± 40	[5920–5740], 5800	Dark brown peat with sand

brown peat that dates back to the Middle-Late Holocene (Table 1). It is possible to assume that such a young age for this altitude is a consequence of a considerable time gap between the drainage of the basin and the subsequent formation of the sediments. The basal core sands are barren of diatoms. Higher up the section, in the peat, rare bog species Eunotia spp. and Pinnularia spp. are noted. Thus, the data of diatom analysis from this core confirm freshwater conditions.

DISCUSSION

Paleogeographic environments during the formation of ancient coastlines

Lithology and wave climate conditions often play a decisive role in the formation of different coastal types. Waves, winds, and currents are the primary drivers of coastal processes. In this case, the presence of a sediment cover and its degree of resistance to coastal erosion are also critical factors influencing coastal evolution (Zenkovich 1967; Bird 2008). In general, glacial and less often glaciofluvial deposits of the Late Valdai glaciation (the last glaciation of the East European Plain) form the basis of coastal landforms in the White Sea (Safianov and Solovieva 2005). Nevertheless, the thickness of the Quaternary deposits within Kandalaksha Bay is relatively small (Astafiev et al. 2012). In places where the bedrocks of the Baltic Shield are exposed, rocky shores resistant to erosion are formed. If there is a cover of loose sediments, the course of coastal processes is primarily governed by wave climate conditions. The Turiy Peninsula in this case represents a good case study where all of the above patterns are observed.

The well-developed series of coastal landforms within the southeastern coast of the Turiy Peninsula were formed as a result of long-term environmental changes such as sea-level change, postglacial uplift (Baranskaya 2018, 2024; Kolka and Korsakova 2017; Korsakova 2022) or wave climate changes (Repkina et al. 2020). Wave climate changes within the White Sea coast can be assessed based on the duration of the ice-covered period (Polyakova et al. 2023). The morphology of coastal landforms can also be used as an indirect indicator of wave climate changes (Kaplin and Selivanov 1999). The interpretation of beach ridges as indicators of depositional or erosional phases is supported by previous research (Zenkovich 1967; Bird 2008) and was used here to reconstruct coastal morphodynamics. Multiple ridges indicate prolonged depositional activity, while gently sloping areas between ridges may signal transitions to erosion-dominated phases.

A morphological criterion for identifying traces of wave reworking (erosional or depositional) of the surface is the presence and regularity of beach ridges (Kaplin and Selivanov 1999). However, this approach provides information only on the relative age of the landforms. In addition, wave-reworked landforms can be destroyed by other erosional processes or by anthropogenic impacts, so some information may be lost. The combination of numerical dating and diatom analysis provides a means to establish the formation age of coastal landforms. Analysis of landform distribution within uplifted land and the modern coastal zone, supported by the results of radiocarbon dating and diatom analysis, allows us to reliably identify a marine-reworked geomorphological level of the uplifted coast up to 26.5 m a.s.l. (calculated as the top of core 160 minus the peat thickness). We also assume that the marine basin did not reach altitudes above 90 m a.s.l. due to the absence of coastal landforms as well as marine diatoms in core 619. Geomorphological levels are identified based on landform characteristics. Below, we provide descriptions of the morphology of each identified geomorphological level and relate their formation to known stages of paleogeographic changes that could have influenced wave dynamics in the area. In this way, we can approximately estimate the ages of geomorphological levels for which numerical dating is not available.

At altitudes of more than 90 (100) m a.s.l., a discontinuous cover of glacial and glaciofluvial deposits is developed (Astafiev et al. 2012; Kolka et al. 2013), which is "washed away" at lower altitudes and reworked by coastal erosion. During our field observations and interpretation of the satellite images, we did not find any traces of wave reworking of landforms elevated above 90 m a.s.l. However, according to other data (Kolka et al. 2013), 3 beach ridges were found at the altitude of 103 m a.s.l. Hence, we can conclude that they occur sporadically. There is an assumption (Kolka et al. 2013) that such high beach ridges and terraces may correspond to coastlines of a former proglacial lake. Further evidence for this is the mosaic pattern of such landforms. Thus, formation of this level corresponds to harsh climatic and glacial conditions of the early stages of deglaciation (Kolka et al. 2013; Polyakova et al. 2023). However, we cannot assert this confidently.

At elevations of 90–70 m a.s.l., we identified sporadic beach ridges on the southeastern slope of Letnyaya Mountain up to 90 m (Fig. 3) during our investigations. These landforms record a phase of coastal processes at this level. Formation of these beach ridges likely occurred after the deglaciation of the peninsula, i.e., later than ~12.5 cal ka BP (Astakhov et al. 2016), under conditions of rapid RSL fluctuations during the Late Glacial transgression (~13.4–11.6 cal ka BP) and regression of the Early Holocene (~11.6–9.5 cal ka BP) (Korsakova 2022). During this period (~13.5–11.5 cal ka BP), the White Sea experienced rapid changes in hydrological conditions (Polyakova et al. 2014). Starting from ~11.7 cal ka BP, a strong current transporting modified Atlantic waters along the Tersky Coast to Kandalaksha Bay became well established (Polyakova et al. 2023). With the ongoing deglaciation, the climate gradually warmed.

Climate warming is also evidenced by reconstructions derived from terrestrial archives. Younger Dryas – early Holocene vegetation in the southern Kola Peninsula consisted of forest-tundra communities with dwarf birches (Elina et al. 2000; Kotlyakov et al. 2014), that were subsequently replaced by birch forests. Since ~10 cal ka BP, pine forests indicative of warm and humid conditions became common (Kremenetski and Patyk-Kara 1997; Sapelko 2009; Grekov et al. 2013b). A warming climate and less extensive sea ice cover facilitated the activation of coastal processes reflected in morphology at this level.

Beach ridges at *70–50 m a.s.l.* are more frequent and have better preservation than those at higher altitudes. Judging from the surface morphology, the landforms at this level were transformed by the sea with more intense wave action and less extensive seasonal sea-ice cover compared to the present conditions. Marine deposits are characterized by poorer sorting compared to those at lower levels. According to the reconstructions by Polyakova et al. (2023), this sea basin likely existed from ~8.6 to 6 cal ka BP (Polyakova et al. 2023), during the Tapes transgression (Korsakova 2022). Paleolandscape reconstructions along the Tersky Coast (Lake Berkut surroundings) indicate that the Turiy Peninsula area may have experienced relatively warmer and more humid than present conditions during this period until 7 cal ka BP (MacDonald et al. 2000; Ilyashuk et al. 2005). This is also confirmed by reconstructions from the area adjacent to the Turiy Peninsula – the Lake

Kanozero area, where middle taiga landscapes were common (Sapelko et al. 2022).

Recent reconstructions (Ludikova et al. 2022) suggest that the level of the Late Glacial transgression exceeded 52.7 m a.s.l. within Kanozero Lake, while on the Turiy Peninsula, the morphology of the beach ridges at elevations of 50–70 m a.s.l. identifies this level as part of the warm sea of the Tapes transgression (9.5–6.8 cal ka BP).

Surfaces below 50 m a.s.l. morphologically resemble modern coastal landforms. We confirm that terraces of this geomorphological level formed at the end of the Middle-Late Holocene (probably later than 6 cal ka BP) based on the obtained data and available reconstructions (Polyakova et. al. 2023). Apparently, the landforms were formed under conditions characterized by seasonal sea-ice cover of short duration. This led to the activation of wave processes. Episodes of high wave activity during this period were also reconstructed in other areas of the White Sea (Nevesskii et al. 1977; Zaretskaya 2018; Repkina et al. 2020), and are indirectly confirmed by the morphology of the Turiy Peninsula coast. The highest and most frequent beach ridges are found within this level (Fig. 3).

Terrestrial climate conditions gradually shifted from the warmest during the Holocene climate optimum towards modern-like. Some cooling occurred at the boundary of the Middle and Late Holocene (Elina et al. 2000). Northern taiga and bogs were widespread in the area of the Turiy Peninsula in association with the slight climate cooling (Sapelko et al. 2022), whereas the waters of the White Sea remained sufficiently warm (Polyakova et al. 2023). Since 1.5 cal ka BP, vegetation assemblages have become similar to modern communities (Elina et al. 2000; Kotlyakov et al. 2014).

The results of radiocarbon dating, lithological, and diatom analyses of sediments from the isolated basins (cores 160 and 99) allowed us to date the coastline positions at 29.5 and 21.5 m a.s.l. (Fig. 6, Table 1). Changes in sediment composition, as well as transitions in the taxonomic composition of diatoms within these basins, probably confirm the existence of residual water bodies in the past. The transition of diatom associations in these basins was probably influenced by both changes in salinity and alterations in the hydrodynamic regime during the isolation of a water body. Judging by the obtained age estimations, the separation of these reservoirs from the sea occurred approximately 4420–3810 cal yrs BP (160/3, Table 1) at 29.5 m a.s.l. and earlier than 3640–3330 cal yrs BP (99/4, Table 1) at 21.5 m a.s.l.

Our results also demonstrate that three morphologically distinct coastal sectors existed throughout the postglacial regional history – the wave-dominated southeastern, primary southern (without traces of wave processes) and tidal northwestern ones (Fig. 3). Modern coastal landforms share the same genetic origin as the uplifted landforms. Based on this, we conclude that changing paleogeographic conditions during the postglacial period had virtually no effect on the morphology of the northwestern coast. Thus, we can conclude that shore exposure to the prevailing wave direction is crucial for its evolution. The presence of loose sediments is equally important in shaping the general appearance of the coast. They provide the material necessary for the formation of coastal landforms, and in their absence, distinct coastal relief cannot form. A clear example of this is the rocky southern coast: although its position is favorable for wave action and it could potentially develop coastal landforms, it contains virtually no landforms due to the absence of loose sediments. Using the Turiy Peninsula as a case study, a notable transition from wave-dominated to tide-dominated coasts, as exposure shifted to the prevailing wave direction along the coastline, was clearly observed for the first time in the White Sea region.

Postglacial movements

The postglacial evolution of the White Sea has been largely shaped by spatially variable glacioisostatic uplift and ongoing neotectonic activity within its basin, reflecting complex interactions between glacial unloading, isostatic adjustment, and regional tectonics. Tectonic movements across the Baltic Shield exhibit a block-structured pattern (Nikonov 1964; Shvarev 2022; Baranskaya 2024). Different movement rates are reported for individual tectonic blocks (Repkina and Romanenko 2016; Kolka and Korsakova 2017; Korsakova 2022). For instance, along the Karelian Coast of the White Sea, differences in uplift rates of up to 5–6 mm/year between macroblocks have been documented (Baranskaya et al. 2019).

The results of radiocarbon dating and diatom analysis allowed us to estimate the Turiy Peninsula uplift rate for the last ~3.5–4 cal ka at 5–7 mm/year. This value significantly exceeds the estimated uplift rate in the adjacent Umba settlement, where rates of ~3.8 mm/year have been reported for the same period (our calculations based on Kolka et al. (2013a)). These results support the interpretation of block-structured tectonic uplift across the Turiy Peninsula.

The stark contrast in uplift rates between adjacent regions highlights the importance of local tectonic configuration and the underlying lithospheric response to deglaciation. Such spatial variability underscores the need for high-resolution reconstructions when interpreting coastline displacement patterns. These differential uplift rates are also consistent with the distribution and preservation of coastal landforms across different altitudes, suggesting a close link between neotectonic activity and morphogenesis. Understanding these localized uplift dynamics is crucial for refining regional RSL curves. Therefore, the Turiy Peninsula exemplifies how postglacial tectonic block movement can significantly alter coastal evolution trajectories even at local scales (Baranskaya et al. 2019).

CONCLUSIONS

This study identified four geomorphological levels on the Turiy Peninsula, distinguished by their elevation, age, and formation conditions:

a. At altitudes above 90–100 m a.s.l., no clear coastal landforms were identified.

b. Landforms at 70–90 (100) m a.s.l. likely formed under conditions of rapid RSL fluctuations during the Late Glacial transgression and Early Holocene regression.

c. The coastal zone at 50–70 m a.s.l. was shaped by a relatively ice-free sea that existed from ~8.6 to 6 cal ka BP.

d. Surfaces below 50 m a.s.l. were formed in the Middle-Late Holocene, likely after ~6 cal ka BP, according to the data from adjacent areas. Their formation reflects conditions increasingly similar to the modern environment. Our paleogeomorphological reconstructions, supported by radiocarbon dating and diatom analysis, confirm their marine origin at elevations up to 26.5 m a.s.l. for the period prior to ~3.5–4 cal ka BP.

The Turiy Peninsula can be divided into three morphologically distinct coastal sectors: a wave-dominated southeastern coast, a southern coast lacking evidence of wave activity, and a tide-influenced northwestern coast.

The topography of uplifted land generally reflects the spatial distribution of modern coastal types. This indicates that modern coastlines inherit their morphology from earlier paleogeographic conditions. Where unconsolidated sediments are present, coastal type is primarily controlled by exposure to prevailing wave directions; where such sediments are absent, bedrock lithology becomes the dominant factor.

The identified geomorphological levels correspond to the key stages in the postglacial evolution of the peninsula. Rapid postglacial uplift was the primary driver shaping the current distribution of coastal landforms. The coastline emerged rapidly from the zone of active wave influence, which limited the reworking of older coastal landforms.

The uplift rate of the Turiy Peninsula (5–7 mm/year over the last ~3.5–4 cal ka) exceeds those of the surrounding areas, supporting the hypothesis of block-structured tectonic behavior in the region.

The Turiy Peninsula example highlights that coastal morphology is primarily shaped by wave exposure and substrate availability. When exposure to wave energy decreases, the coastline rapidly transitions into a tide-dominated regime. ■

REFERENCES

Arkhipkin V.S., Dobrolyubov S.A., Myslenkov S.A. and Korablina A.D. (2015). The waves climate of the White Sea. In: S.A. Sokratov, ed., Changing climate and socio-economic potential of the Russian Arctic: Arctic seas and islands, Moscow: Liga-Vent, Lomonosov Moscow State University, Faculty of Geography, 48-58 (in Russian).

Astafiev B.Yu., Bogdanov Yu.B., Voinova O.A., Voinov A.S., Gorbatsevich N.R., Zhuravlev V.A., Nogina M.Yu., Paramonova M.S., Proskurin G.Yu., Rybalko A.E., Semenova L.R., Surikov S.N. and Shkarubo S.I. (2012). State Geological Map of the Russian Federation, 1:1 000 000, 3rd Generation, Baltic Series, Sheet No. Q-(35), 36 – Apatity, Explanatory Note. St. Petersburg: Kartograficheskaya fabrika A.P. Karpinsky Russian Geological Research Institute (in Russian).

Astakhov V., Shkatova V., Zastrozhnov A. and Chuyko M. (2016). Glaciomorphological map of the Russian Federation. Quaternary International, 420, 4-14, DOI: 10.1016/j.quaint.2015.09.024.

Baranskaya A.V., Khan N.S., Romanenko F.A., Roy K., Peltier W.R. and Horton B.P. (2018). A postglacial relative sea-level database for the Russian Arctic coast. Quaternary Science Reviews, 199, 188-205, DOI: 10.1016/j.quascirev.2018.07.033.

Baranskaya A.V., Maznev S.V., Romanenko F.A. and Shilova O.S. (2019). Recent crustal movements of the Karelian coast of the White Sea. Arktika i Antarktika, 2, 16-33 (in Russian), DOI: 10.7256/2453-8922.2019.2.29635.

Baranskaya A.V. (2024). The Russian part of the Baltic crystalline shield: recent uplift of one of the Earth's most ancient massives. Doklady Earth Sciences, 519 (1), 26-40, DOI: 10.1134/S1028334X24604991.

Bird E.C.F. (2008). Coastal geomorphology: an introduction. Chichester, Hoboken, NJ: Wiley.

Davydova N.N. (1985). Diatoms as indicators of the natural conditions of reservoirs in the Holocene. Leningrad: Nauka (in Russian).

Demidov I.N., Houmark-Nielsen M., Kjær K. H. and Larsen E. (2006). The last Scandinavian Ice Sheet in northwestern Russia: ice flow patterns and decay dynamics. Boreas, 35, 339-354, DOI: 10.1080/03009480600781883.

Diatoms of the USSR, fossil and modern. (1974). Vol. 1. Leningrad: Nauka (in Russian).

Donner J., Eronen M. and Jungner H. (1977). The dating of the Holocene relative sea-level changes in Finnmark, North Norway. Norsk Geografisk Tidsskrift, 31, 103-128, DOI: 10.1080/00291957708552013.

Elina G.A., Lukashov A.D. and Yurkovskaya T.K. (2000). Late glacial and Holocene of Eastern Fennoscandia (paleovegetation and paleogeography). Petrozavodsk: KarNTs Ross. Akad. Nauk (in Russian).

ESIMO, (2007). Atlas «Climate of the seas of Russia and key areas of the World Ocean»: White Sea. (online) Available at: https://www.esimo.ru/atlas/index_atlas.html (Accessed 1 May 2025).

Evzerov V.Ya., Korsakova O.P. and Kolka V.V. (2007). Evolution of marine basins in the White Sea depression over the past 130 thousand years (state of the issue and research prospects). Bull. Komissii po izucheniyu chetvertichnogo perioda, 67, 36-42 (in Russian).

Grekov I.M., Zaretskaya N.E. and Kolka V.V. (2013a). The Early Holocene deposits of the Kuzreka River Valley. In: G.G. Matishov, ed., Fundamental problems of Quaternary, results and main trends of further studies: Proceedings of the VIII All-Russian conference on Quaternary research, Rostov-on-Don: YuNTs RAN, 151-152 (in Russian).

Grekov I.M., Syrykh L.S., Kosheleva E.A. and Subetto D.A. (2013b). Paleolandscapes of the early Holocene of the Kola Peninsula and geoarchaeology. Society. Environment. Evolution, 3, 275-282 (in Russian).

Guiry M.D. and Guiry G.M. (2025). AlgaeBase. World-wide electronic publication, University of Galway (online) Available at: https://www.algaebase.org (Accessed 10 Feb. 2023).

Hughes A.L.C., Gyllencreutz R., Lohne Ø.S., Mangerud J. and Svendsen J.I. (2016). The last Eurasian ice sheets e a chronological database and time-slice reconstruction, DATED-1. Boreas, 45(1), 1-45, DOI: 10.1111/bor.12142.

Hustedt F. (1957). Die Diatomeenflora des Flußsystems der Weser im Gebiet der Hansestadt Bremen. Abhandlungen des Naturwissenschaftlichen Verein zu Bremen, 34(3), 181-440.

Ilyashuk E.A., Ilyashuk B.P., Hammarlund D. and Larocque I. (2005). Holocene climatic and environmental changes inferred from midge records (Diptera: Chironomidae, Chaoboridae, Ceratopogonidae) at Lake Berkut, southern Kola Peninsula, Russia. The Holocene, 15(6), 897-914, DOI: 10.1191/0959683605hl865ra.

Kagan L.Ya. (2012). Diatom algae of the Euro-Arctic region. Annotated collection (ancient and modern marine and freshwater). Apatity: KNTs RAN (in Russian).

Kaplin P.A. and Selivanov A.O. (1999). Sea-level changes in Russia and coastal development: past, present, future. Moscow: GEOS (in Russian).

Kaplin P.A., Leontiev O.K., Lukyanova S.A. and Nikiforov L.G. (1991). Coasts. Moscow: Mysl' (in Russian).

Kolka V.V., Evzerov V.Ya, Møller J.J. and Corner G.D. (2013). Late Pleistocene-Holocene sea level changes and bottom sediment stratigraphy of isolated lakes in the southern Kola Peninsula, area of Umba settlement. Izv. RAS Ser.Geogr., 1, 73-88 (in Russian), DOI: 10.15356/0373-2444-2013-1-73-88.

Kolka V.V., Korsakova O.P., Shelekhova T.S. and Tolstobrova A.N. (2015). Reconstruction of the relative level of the White Sea during the Lateglacial – Holocene according to lithological, diatom analyses and radiocarbon dating of small lakes bottom sediments in the area of the Chupa settlement (North Karelia, Russia). Vestnik of MSTU, Proceedings of the Murmansk State Technical University, 18(2), 255-268 (in Russian), DOI: 10.7868/S0869592X16030042.

Kolka V.V., Korsakova O.P., Tolstobrova A.N., Tolstobrov D.S., Lavrova N.B. and Shelekhova T.S. (2016). Lithology and late postglacial stratigraphy of bottom sediments in isolated basins of the White Sea Coast exemplified by a small lake in the Chupa Settlement area (Northern Karelia). Stratigraphy and Geological Correlation, 24(3), 294-312, DOI: 10.7868/S0869592X16030042.

Kolka V.V. and Korsakova O.P. (2017). The position of the coastline of the White Sea and neotectonic movements in the North-East of Fennoscandia in the Late Glacial and Holocene. In: A.P. Lisitzin, I.A. Nemirovskaya, V.P. Shevchenko et al., eds., White Sea system. Volume IV. Sedimentation processes, geology and history, Moscow: Nauchnyi Mir, 222-249 (in Russian).

Korsakova O.P. (2022). White Sea coasts within Fennoscandian crystal Shield in the Neopleistocene and Holocene. Izvestiya RAN. Ser. Geogr., 86(6), 883-897 (in Russian), DOI: 10.31857/S258755662206005X.

Korsakova O.P., Vashkov A.A. and Nosova O.Yu. (2023). European Russia: Glacial landforms from the Younger Dryas stadial. In: D. Palacios, P.D. Hughes, J.M. Garcia-Ruiz et al., eds., European Glacial Landscapes. The Last Deglaciation, Amsterdam, Oxford, Cambridge: Elsevier, 467-472, DOI: 10.1016/B978-0-323-91899-2.00014-0.

Koshechkin B.I. (1979). Holocene Tectonics of the Eastern Part of the Baltic Shield. Leningrad: Nauka (in Russian).

Kremenetski C.V. and Patyk-Kara N.G. (1997). Holocene vegetation dynamics of the southeast Kola Peninsula, Russia. The Holocene, 7, 473-479, DOI: 10.1177/095968369700700409.

Lavrova M.A. (1960). Quaternary Geology of the Kola Peninsula. Moscow-Leningrad: USSR Academy of Sciences Press (in Russian).

Letanskaya G.I. (1974). Phytoplankton and primary production of the Kola Peninsula lakes. In: Lakes in different landscapes of the Kola Peninsula, Leningrad, Part 2, 78-119 (in Russian).

Ludikova A.V., Sapelko T.V. and Kuznetsov D.D. (2022). On the marine limit at the Kandalaksha Coast, the White Sea: new data from Lake Kanozero, a huge isolation basin in the middle course of the River Umba. Limnology and Freshwater Biology, 4, 1473-1475, DOI: 10.31951/2658-3518-2022-A-4-1473.

MacDonald G.M., Velichko A.A., Kremenetski C.V., Borisova O.K., Golyeva A.A., Andreev A.A., Cwynar L.C., Riding R.T., Forman S.L., Edwards T.W.D., Aravena R., Hammarlund D., Szeicz J.M. and Gattaulin V.N. (2000). Holocene treeline history and climate change across Northern Eurasia. Quaternary Research, 53(3), 302-311, DOI: 10.1006/qres.1999.2123.

Nevesskii E.N., Medvedev V.S. and Kalinenko V.V. (1977). The White Sea. Sedimentogenesis and History of Development in the Holocene. Moscow: Nauka (in Russian).

Nikiforov S.L., Koshel S.M. and Frol V.V. (2012). Digital terrain model of the White Sea bottom. Vestnik Moskovskogo universiteta. Seriya 5. Geografiya, 3, 86-92 (in Russian).

Nikonov A.A. (1964). Relief evolution and paleogeography of the Anthropogene in the west of the Kola Peninsula. Moscow-Leningrad: Nauka (in Russian).

Nikulina V.N. (1975). Phytoplankton. In: G.G. Vinberg, ed. Biological Productivity of the Northern Lakes, Part 1. Lakes Krivoe and Krugloe, Leningrad: Nauka, 42-54 (in Russian).

Polyakova Y., Agafonova E., Novichkova E. and de Vernal A. (2023). Holocene paleoenvironmental implications of diatom, non-pollen palynomorph, and organic carbon records from the Kandalaksha Bay of the White Sea (European Arctic). Geosciences 13, 2-23, DOI: 10.3390/geosciences13020056.

Porter C., Howat I., Noh M-J., Husby E., Khuvis S., Danish E., Tomko K., Gardiner J., Negrete A., Yadav B., Klassen J., Kelleher C., Cloutier M., Bakker J., Enos J., Arnold G., Bauer G., Morin P. (2023). ArcticDEM, Version 4.1. (online). Available at: www.pgc.umn.edu (Accessed 30 Jan. 2025).

Reimer P.J., Austin W.E.N., Bard E., Bayliss A., Blackwell P.G., Bronk Ramsey C., Butzin M., Cheng H., Edwards R.L., Friedrich M., Grootes P.M., Guilderson T.P., Hajdas I., Heaton T.J., Hogg A.G., Hughen K.A., Kromer B., Manning S.W., Muscheler R. and Talamo S. (2020). The IntCal20 Northern Hemisphere Radiocarbon Age Calibration Curve (0–55 cal kBP). Radiocarbon, 62(4), 725-757, DOI: 10.1017/RDC.2020.41.

Repkina T.Yu, Shilova O.S., Krasnova E.D., Entin A.L., Grigoriev V.A., Vakhrameyeva E.A., Losyuk G.N., Kublitskiy Yu.A., Leontiev P.A., Lugovoy N.N., Voronov D.A. and Frolova N.L. (2023). From the sea strait to the meromictic lake: Evolution and ecosystem of a water body at the Fiard Coast (Lake Kislo-Sladkoe at the Karelian Coast of the Kandalaksha Bay, the White Sea, Russia). Quaternary International, 644-645, 122-137, DOI: 10.1016/j.quaint.2022.05.015.

Repkina T.Yu. and Romanenko F.A. (2016). Coastal relief of the Babye Sea and the Velikiy Island: history of development and modern changes. Proceedings of the White Sea Biological Station of Lomonosov Moscow State University, 12, 170-210 (in Russian).

Repkina T.Yu., Romanenko F.A., Ludikova A.V. and Zaretskaya N.E. (2020). The northwestern shores of the Onega Peninsula of the White Sea in the Holocene: development conditions, dynamics, chronology. Izvestiya RAN. Seriya Geograficheskaya, 84(6), 888–904 (in Russian), DOI: 10.31857/S2587556620060096.

Safianov G.A. and Solovieva G.D. (2005). Geomorphology of the bottom and coasts of the White Sea. Moscow University Bulletin. Series 5, Geography, 3, 54-62 (in Russian).

Sapelko T. V., Ludikova A. V., Shumkin V. Ya., Kuznetsov D. D. and Subetto D. A. (2009). Changes in natural environments of the southern part of the Kola Peninsula in the late post-glacial period. Fundamental problems of the Quaternary, results and main trends of further studies: proceedings of VI All-Russian conference on Quaternary research, October 19-23, 2009, Novosibirsk, Novosibirsk Branch of the RAS, 534-537. (in Russian).

Sapelko T.V., Kuznetsov D.D., Ludikova A.V., Kolpakov E.M. and Shumkin V.Y. (2022). Late Glacial – Holocene history of the Lake Kanozero in the southern Kola Peninsula, northwestern Russia. Geomorfologiya, 3, 29-38, DOI: 10.31857/S0435428122030154. (in Russian).

Shilova O.S., Zaretskaya N.E. and Repkina T.Yu. (2019). Holocene deposits of the southeastern coast of the Gorlo strait (White Sea): New data of diatom and radiocarbon analyses. Doklady Earth Sciences, 488(2), 1259-1263, DOI: 10.1134/S1028334X19100258.

Stroeven A.P., Hättestrand C., Kleman J., Heyman J., Fabel D., Fredin O., Goodfellow B.W, Harbor J.M., Jansen J.D., Olsen L., Caffee M.W., Fink D., Lundqvist J., Rosqvist G.C., Strömberg B. and Jansson K.N. (2016). Deglaciation of Fennoscandia. Quaternary Science Reviews, 147(6), 91-121, DOI: 10.1016/j.quascirev.2015.09.016.

Shvarev S.V. (2022). Morphotectonics, seismicity, and exogenous processes of the Kola Peninsula. Russian Geology and Geophysics, 63(8), 940-954, DOI: 10.2113/RGG20204310.

Subetto D.A. (2009). Lake Bottom Sediments: Paleolimnological Reconstructions. St. Petersburg: RGPU. (in Russian).

Terziev F.S., Goptarev N.P., Kalatsky V.I., Simonov A.I., Borisenko M.M., Borodachev V.E. Gershanovich D.E., Girdyuk G.V., Kerimov A.A., Kolesnichenko N.N., Rozhkov V.A., Fedorei V.G. (Eds.). (1991). Hydrometeorology and Hydrochemistry of the Seas of USSR, Vol. II: The White Sea. Leningrad: Gidrometeoizdat. (in Russian).

Weckström K. and Juggins S. (2005). Coastal diatom-environment relationships from the Gulf of Finland, Baltic Sea. Journal of Phycology, 42(1), 21-35, DOI: 10.1111/j.1529-8817.2006.00166.x.

Witkowski A., Lange-Bertalot H. and Metzeltin D. (2000). Diatom flora of marine coasts I. Iconographia Diatomologica, Vol.7.

Yermolov A.A. (2010). Geomorphology of the Kola Peninsular shores in the White Sea. Geomorphology, 1: 36-42, DOI: 10.15356/0435-4281-2010-1-36-42. (in Russian).

Zaretskaya N.E. (2018). The Holocene history of the North Dvina River delta. Geomorfologiya, 1, 3-17, DOI: 10.7868/S0435428118010017. (in Russian).

Zaretskaya N.E., Ponomareva V.V. and Sulerzhitsky L.D. (2007). Radiocarbon dating of large Holocene volcanic events within South Kamchatka (Russian Far East). Radiocarbon, 49, 2, 1065-1078, DOI: 10.1017/S0033822200042922.

Zaretskaya N.E., Ponomareva V.V., Sulerzhitsky L.D. and Zhilin M.G. (2001). Radiocarbon studies of peat bogs: an investigation of South Kamchatka volcanoes and Upper Volga archeological sites. Radiocarbon, 43, 2, 138-147, DOI: 10.1017/S0033822200041229.

Zenkovich V. P. (1962). Fundamentals of the doctrine of the development of sea coasts. Moscow: Academy of Sciences of the USSR. (in Russian).

Zenkovich V. P. (1967). Processes of coastal development. New York: Interscience Publishers.